WIRELESS MONITORING OF INTERNAL WOUND ROLL PRESSURES

By

Timothy J. Walker[1] and Robert C. Updike[2]
[1] TJWalker+Associates Inc.
[2]Optimation Technology, Inc.
USA

ABSTRACT

Winding is a dynamic process. The final roll is the product of all that happens during the winding process from roll start to final cutoff. Nearly all roll measurement methods try to characterize a roll's structure after winding is completed, like understanding why a plane crashes from diagnosis of the debris. What winding needs is the equivalent of a 'black box,' a monitoring device to record the dynamic nature of the winding process. Using thin resistance-based pressure sensors and wireless data collection, we will show the changes inside a winding roll as a function of key winding variable, including product properties, winding torque and nip loads, winding speed, and rotation position.

NOMENCLATURE

$T_{NCW,WOT}$ = Tension of Nipped Center Winding, force per width

T_{WH} = Tension of Web Handling upstream of winding, force per width

μ_K = Kinetic coefficient of friction web side A to B, dimensionless

N_x = Nip load at radial position r_x, force per width

r_x = Radius, length

$P_{CORE,CUM}$ = Cumulative Pressure at the roll's core, force per area

MOTIVATION OF WORK

Historically, winding process research has been confirmed by measuring internal roll pressures after winding is complete[1,2,3]. This approach fails to capture the dynamic effects within a winding roll, such as slippage and roll rotation. A limited number of dynamic internal roll pressure measurements have used strain gauges on steel or aluminum cores,

but this approach is insulated by the core wall thickness and cannot detect the small pressure variations from the winding nip roller contact, core imperfections, or narrow gauge bands.

Many winding defects have complicated mechanisms that have proven elusive to winding models. Real-world winding includes uneven nipping contact, wrinkled roll starts, and core compression and deflection. These imperfections are rarely included in winding models, yet contribute greatly to waste to converting processes.

One of the most common winding defects, cinching-induced telescoping is typically under-predicted from winding models where internal friction and torque transmission capacity is almost always over-estimated. One possible explanation for cinching to occur before models predict is the 'internal nip' created by gravity in core-supported winding.

The 'internal nip' is especially significant for products with:

- Large buildup ratios (Rfinal/Rcore)
- Low core pressure (common in paper winding)
- High density
- Roll weight supported by the core (via shafts of chucks)

The rotation of the near-core layers passing through the 'internal nip pressure' of the roll weight over the area of the core cross-section is suspected as a near-core layer loosening effect.[4,5]

EXPERIMENTAL SETUP AND RESULTS

To measure near-core roll pressure during the winding process, thin film pressure sensors were inserted in the layers near the core and tethered to a wireless data transmitter to send the roll pressure data to a nearby computer over Wi-Fi frequencies.

The properties of the thin-film pressure sensors are listed in the following table:

Sensor Property	
Linearity	<±3%
Repeatability	<±3.5%
Hysteresis	< 4.5% of full scale
Drift per log time	5%
Lag Time	5 µsec
Operating Temperature	15° to 140°F (-9° to 60°C)
Thinness	0.004 in (0.1 mm)
Sensel Density	Up to 1,600 per sq. in. (248 per sq. cm) Pitch as fine as 0.025 in. (0.6 mm)
Pressure Range	Up to 30,000 psi (207 MPa) (dependent on sensor selection)

Table 1 – Pressure Sensor System Performance per Manufacturer

Pressure Sensor and System Calibration

The thin film pressure sensors require calibration to convert resistance measurements into pressure. Figure 3 shows the calibration method using dead weights.

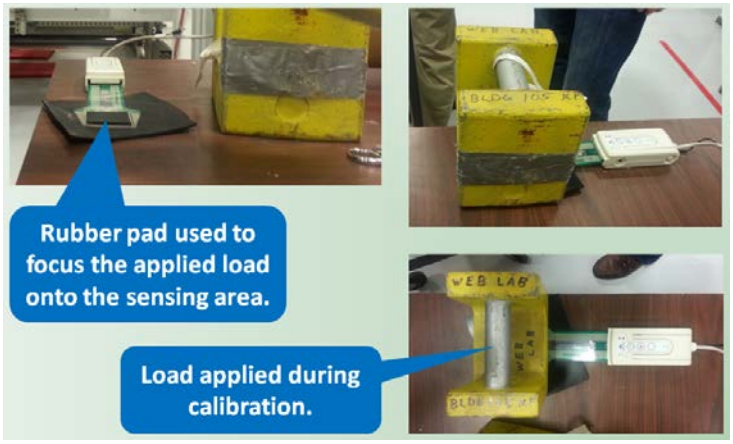

Figure 1 – Sensor calibration

Experimental Setup #1

Figure 2 shows the components and initial layout of our wireless pressure measurement system mounted on an extended 3-inch paper core.

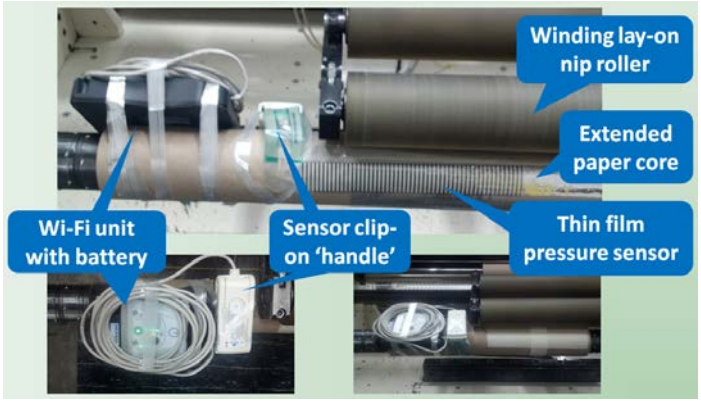

Figure 2 – Equipment Setup #1 for 75mm (3-in) Core

The pressure mapping software allows analysis by time and position. In an early run, a 'movie' of pressure was collected from all 2288 sensels at a rate of 10Hz. The 19 minute run (1152s) collected 26 million data points with a file size of 105Mb.

Experimental Setup #2

- To show the feasibility of mounting the pressure sensor hardware inside a 150mm inner diameter paper core, enabling the use of the system with minimal change to production operations.
- To compare winding with and without a wind nip roller.
- To monitor the core pressure in the unwinding process.

In this second series of experiments, the pressure sensor handle and Wi-Fi transmitter unit were placed inside a 150mm (6-in) paper core. A different smaller sensor was used in this experiment, with a 1936-sensel array over a 84 by 84 mm area (3.3 x 3.3-in), with one sensel point for every 1 x 1 mm area (40 x 40 mils). A large variety of standard and custom sensor sizes, shapes, and pressure ranges are commercially available. These small square sensors were readily available without added cost, but longer transverse or machine direction sensors would provide a more thorough movie of core pressure varitions.

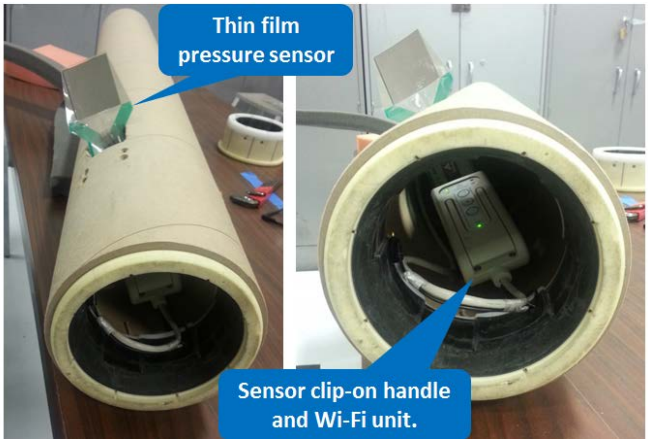

Figure 3 – Experimental Setup #2 for 150mm (6-in) Core

Figure 4 shows the in-core system mounted on the winders. The core is coupled to the winder drive by two end chucks, but no through shaft, similar to many production winders. The pressure measuring end of the sensor is taped to the outside of the core. The connection end of the sensor is routed through a hole in the core, connecting to the handle and Wi-Fi unit tucked inside the core. All the internal system components are far enough from the core end to leave space for the core chucks.

Figure 4 – Equipment on Winder Mounted Inside of Core

Mapping Pressure Over Area

A major advantage of thin-film sensor pressure mapping over other methods is the measurement of pressure over a large area with discrete sensing pixels (sensels) that create a contour map of pressure in the machine and transverse direction over the sensor area. Key process details that are captured with this ability include: pressure and footprint area of nip contact, pressure losses from core imperfections, and pressure variations from gauge bands.

Figure 5 shows the thin-film pressure sensor detecting the line-contact of the winding lay-on nip roller. The top third of the pressure map shows the low pressure before contact with the winding nip roller. The high pressure (lighter band running left to right) line shows the footprint of the winding nip roller. The bottom two-thirds of the pressure map shows the added tension from an additional layers tension created by torque and nip load. Figure 6 shows the nip roller footprint during our second experiment (see the band running top to bottom).

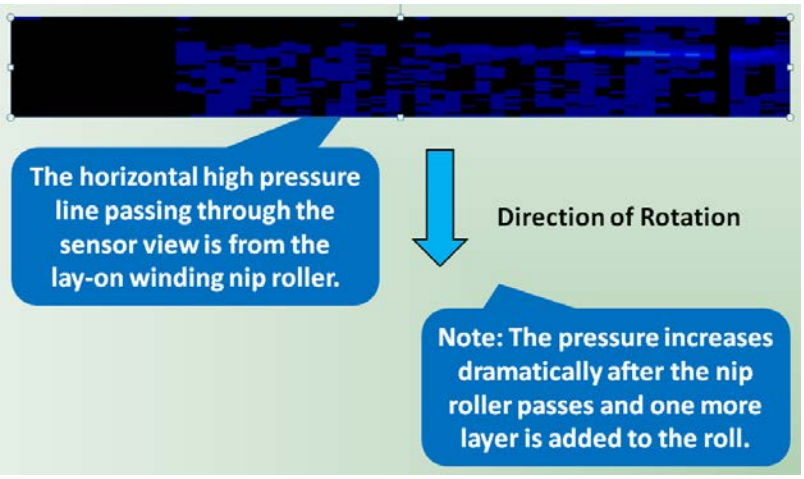

Figure 5 – Experiment #1 Winding Nip Line Contact Mid-Sensor

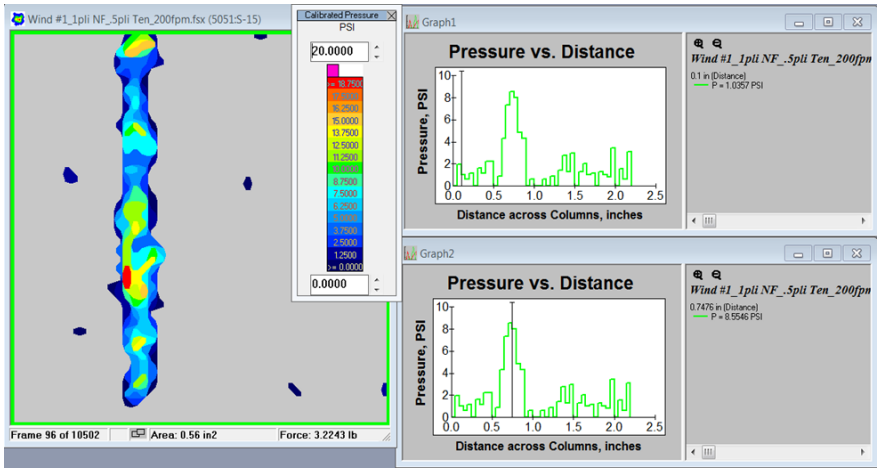

Figure 6 – Experiment #2 Winding Nip Line Contact Mid-Sensor

Figure 7 shows the pressure map towards the end of the winding process. The pressure mapping system detected a diagonal region of near zero pressure. Upon inspection, it was clear this aligned to a gap in an inner layer of the spiral wound core.

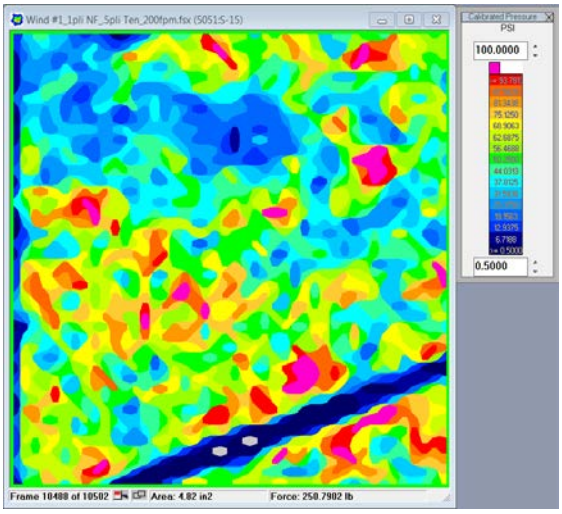

Figure 7 – Core Pressure Map Showing Core Wrap Imperfection

Core Pressure vs. Winding and Unwinding Time

Figure 8 shows the near-core pressure increase over a series of layers added to the winding roll. Each layer shows a starting pressure, a pressure spike from the nip roller contact, a higher pressure after the contact of the winding nip and addition of one layer, then a slight decrease in pressure until the next contact with the pressure roll and next added layer. In this diagram, the time between added layers shifts as winding speed is increased.

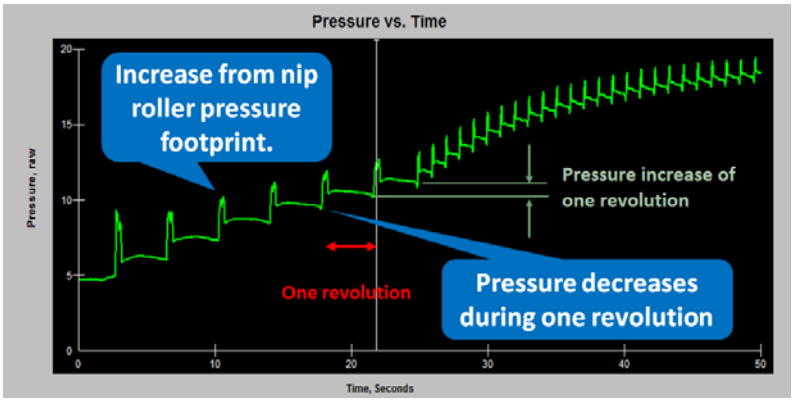

Figure 8 – Pressure vs Time Showing Individual Revolutions

Near-core pressure is predicted to be a function of the tension of each layer added to the winding roll. The pressure of one layer will be the tension (in units of force per width) divided by the roll radius. The tension of an added layer when center winding with a lay-

on nip roller ($T_{NCW,WOT}$) will be a function of web handling tension created by winding torque (T_{WH}) and nip-induced tension created by the nip is proportional to the web's side A to B kinetic coefficient of friction (μ_K) and nip load (N).

$$T_{NCW,WOT} \approx T_{WH} + \mu_K N \quad \{1\}$$

A straight cumulative model, with no account of tension losses from core or roll layer compression, would predict a cumulative core pressure from the sum of pressures created by all the layers tension divided by their radii. Equation 2 calculates the maximum cumulative core pressure from all the layers 1 through i. In our experiments, web handling tension and nip load were held constant as radius increased, but this equation allows for possible tapering of tension or nip load as a function of radius.

$$P_{CORE,CUM} = \sum_1^i \frac{\left(T_{WHx} + \mu_K N_x\right)}{r_x} \quad \{2\}$$

Figure 9 – Film Core Pressure vs Radius, Actual and Cumulative Maximum

Film winding core pressure increases proportional to cumulative tension over radius for the first 50mm or radial buildup (Figure 9). The pressure then increases at a rate slower than cumulative tension over radius due to core and near-core layers radial compression.

Figure 10 – Film and Paper Core Pressure, Actual and Cumulative Maximum

Paper winding core pressure increases proportional to cumulative tension over radius for only 5-10mm (25 s) before reaching a plateau value then, surprisingly, core pressure decreases slightly as the roll continues to build.

The thin-film pressure sensors map more than just average pressure. The pressure data can be analyzed by lateral or rotational position vs. time. The following diagram shows the near-core pressure of a film roll.

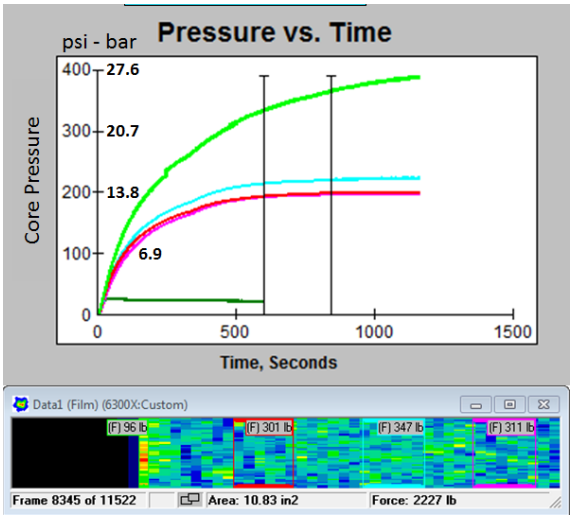

Figure 11 – Film and Paper Winding Core Pressure Increase vs. Lateral Position

Film roll near-core edge pressures were two time higher than non-edge pressures. Film roll near-core pressures, for similar winding conditions, were 5-10x paper roll pressures (Figure 11). Paper roll pressures varied two to one depending on lateral position (Figure 12). The pressure away from the film roll edge plateaus at the mid-point of winding the full roll, but the edge pressure continues to rise with each added layer.

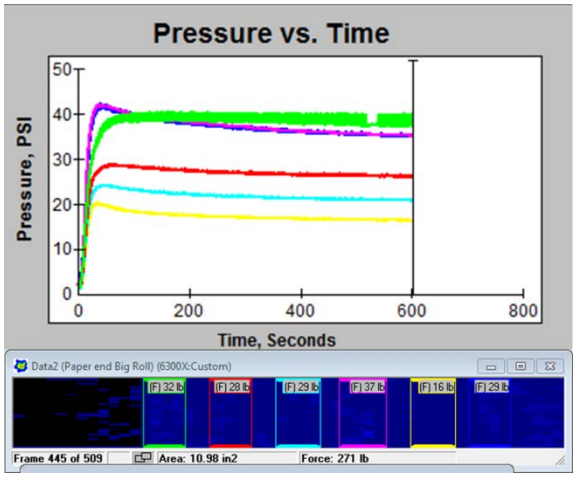

Figure 12 – Paper Roll Core Pressure vs. Lateral Position

Figure 13 (below) shows the buildup of core pressure over time during winding with the in-core system. The three conditions are for winding with a constant tension (85 N/m) and winding nip conditions of high (175N/m), low (85N/m), and no winding nip load. In this set of experiments, the higher winding nip load created only minor increase in core pressure. Most likely this was due to insufficient nip load under either condition to compress the entrained air layer below product surface roughness. The no nip winding case created a wound roll with extremely low core pressure, showing how a high level of air lubrication can release internal tensions and roll pressure.

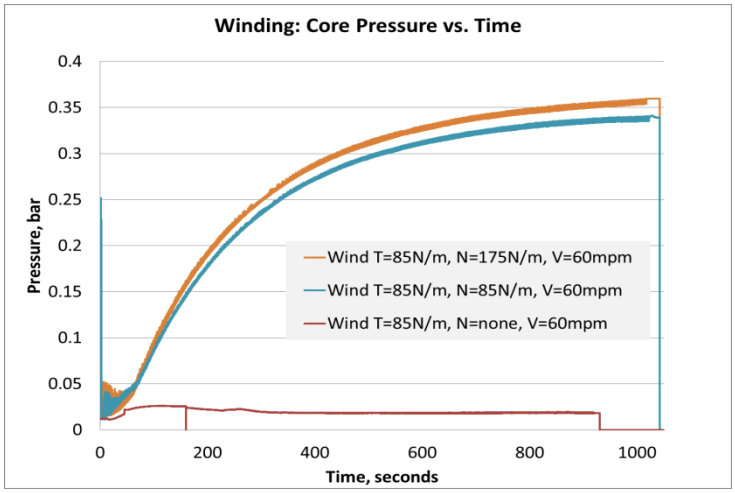

Figure 13 – Winding Core Pressure vs. Time

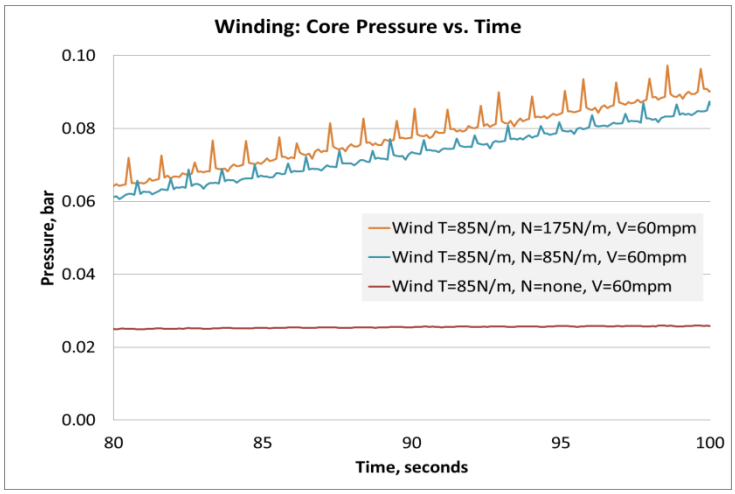

Figure 14 – Winding Core Pressure vs. Time

Figure 14 shows a short time period of the winding process to highlight the pressure buildup per revolution of the winding roll. Note the upward features of the rising core pressure. Each up feature is the temporary core pressure increase from the winding nip roller contact. The core pressure clearly increases with each additional layer of winding. Looking closely at the three curves, the up feature on the higher nip load curve is about two times the size of the low nip load condition; yet, the core pressure is not rising significantly faster with the higher nip load. The no nip winding shows no once per revolution pressure increase.

Figure 15 shows the core pressure during unwinding. The two unwinding core pressure curves show no significant discontinuities, looking like a reversal of the winding core pressure increase plots.

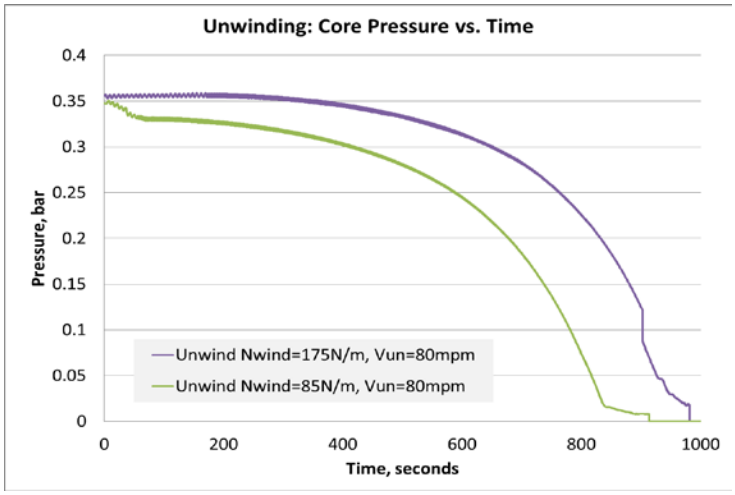

Figure 15 – Unwinding Core Pressure vs. Time

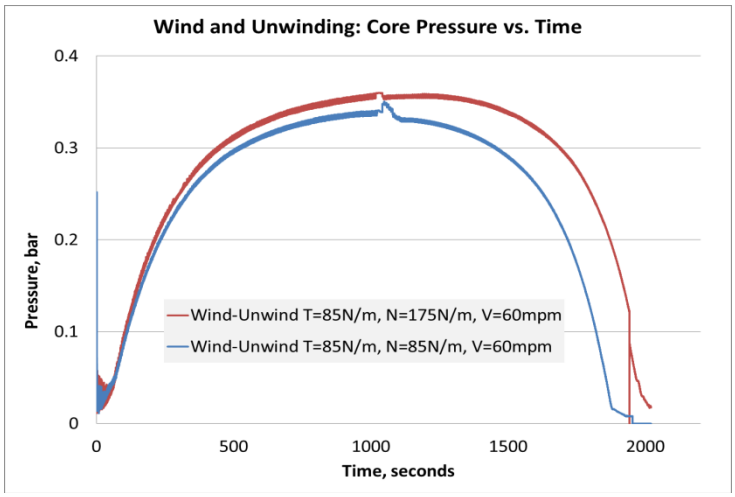

Figure 16 – Combined Winding and Unwinding Core Pressure vs. Time

Figure 16 shows the winding and unwinding plot of two rolls on the same graph. The unwinding occurs over a short time period due to a speed change (winding at 40 mpm and unwinding at 50 mpm). It does appear in the lower curve that the unwinding is not quite a mirror image of the winding process, possibly showing a delay in the release of core pressure as layers are released. The reason for this delayed release of core pressure is not clear, but could be caused by either stick-slip difference between winding and unwinding or other mechanisms that prevent the physical motion and strain change needed to release the winding tension.

Core Pressure vs. Roll Rotation

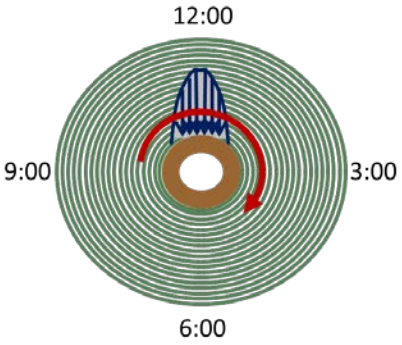

Figure 17 – Rotation-Dependent Core Pressure Variations

In our large paper rolls, the near core pressure was shown to be a strong function of rotation position. When the pressure sensor was at the top (12:00) position of the core, the pressure was higher than when it was at 3:00 or 9:00. When the pressure sensor was at the bottom (6:00) position of the core, the pressure was lower than when it was at 3:00 or 9:00. This rotation-position pressure variation was more significant at the roll's edge.

The near-edge increased sensitivity may be cause by the deflection and geometry of our roll, core, and shaft.

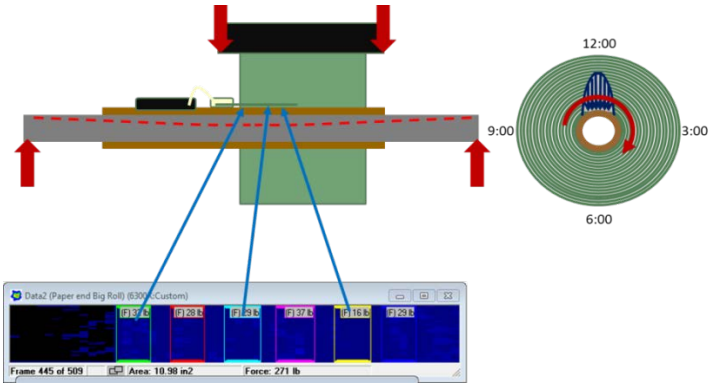

Figure 18 – Cross-Roll Rotation Pressure Variations

Figures 19 and 20 show a detail of the pressure oscillation measured at the core from roll rotation in experiment #2. In Figure 19, the pressure oscillation is 1.4 Hz which corresponds to rotation of the 230mm diameter roll winding at 60 mpm. Figure 20 shows rotational core pressure variations for rolls wound with high and low winding nip load. In the top data curve, the oscillation frequency increases as the unwinding roll is sped up from jog speed to 75 mpm.

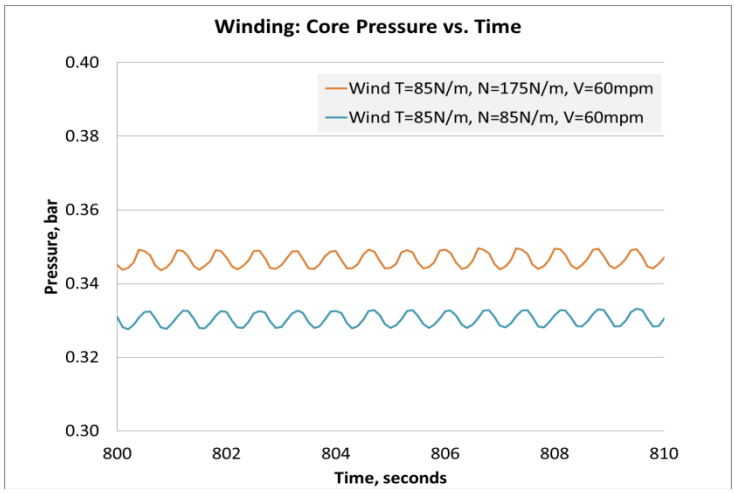

Figure 19 – Winding Core Pressure vs. Time, End of Winding

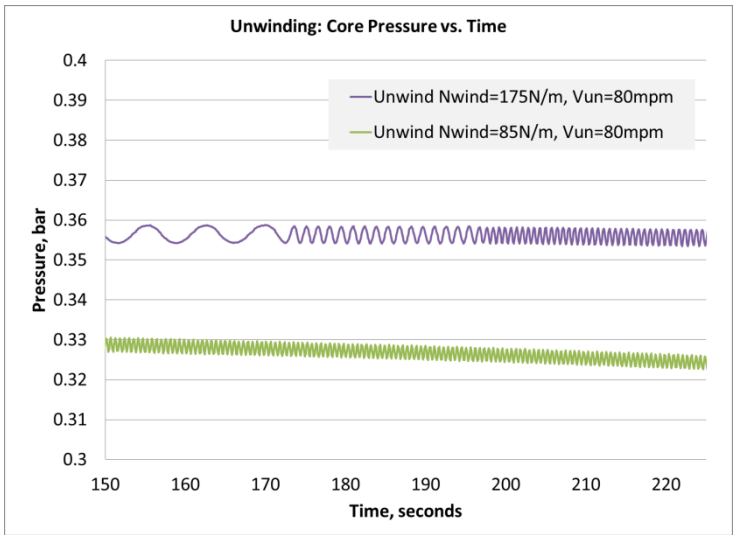

Figure 20 – Unwinding Core Pressure vs. Time, Start of Unwinding

CONCLUSIONS

- Thin tactile pressure sensors and wireless data collection allows a dynamic view of the winding process.
- Near-core winding pressure can be mapped vs. both lateral and rotational position over time.
- This methods provides a 'live' view of the once-per-revolution high pressure footprint from the winding lay-on nip roller.
- The paper and film winding near-core pressures initially increase with a good correlation to cumulative pressure of tension/radius.
- Film winding roll core pressures followed the cumulative pressure curve for many layers, but eventually deviated to lower pressures than the cumulative pressure.

- The 'internal nip' of large diameter, core-supported rolls was verified, showing the effects of gravity on near-core pressure vs. roll rotation.
- Core pressure differ greatly in winding with and without a winding lay-on nip roller.
- Core pressures decreased incrementally over unwinding, at a rate nearly the reverse of the winding process, but with an initial delay in releasing the core pressure.
- The wireless pressure measurement system can be mounted inside a 150mm (6-inch) inner diameter core and survive the rotation of winding at modest speeds (75 mpm, 250 fpm), making is a credible tool for production problem-solving, such as monitoring variations in at-speed roll transfers.

ACKNOWLEDGMENTS

I would like to thank my experiment partners: for experiment #1, Camilo Aladro (Tekscan, South Boston, MA, USA) and Dan Weber (WebCut Converting, Eagan, MN, USA) and for experiment #2, Michael Contrastano (Tekscan) and Tom Rottolo

(Optimation), and to Vincent Carrara (Tekscan) for his continued support of pressure mapping in converting nipped and winding processes. Special thanks to my co-author Robert Updike (Optimation) for his technical support in collecting and analyzing pressure measurement data. This paper, presentation, and experiments would not have been possible without their combined generosity – donating time, equipment, labor, and most of all, their expertise to these experiments. I thank them all for joining me in this venture and seeing the value of exploring winding pressure via wireless measurement.

REFERENCES

1. Hakiel, Z., "On the Effect of Width Direction Thickness Variations in Wound Rolls," Proceedings of the First International Conference on Web Handling, 1991, WHRC, Oklahoma State University, Stillwater, OK, pp. 79-98.
2. Kedl D. M., "Using a Two Dimensional Winding Model to Predict Wound Roll Stresses That Occur Due to Circumferential Steps in Core Diameter or to Cross Web Caliper Variation," Proceedings of the First International Conference on Web Handling, 1991, WHRC, Oklahoma State University, Stillwater, OK, pp. 99-112.
3. Gale, J. W., "Winding Experiments on Nonuniform Thickness Webs," Master's Theses, July 2012, Oklahoma State University, Stillwater, OK.
4. Lucas, R. G., "Internal Gearing in a Roll of Paper," TAPPI Finishing and Converting Conference Proceedings, October 1974.
5. Hussain, S. M. and Farrell, W. R., "Roll Winding — Causes, Effects and Cures of Loose Cores in Newsprint Rolls," TAPPI Journal, Vol. 60, No. 5, May 1977.
6. Frye, K., "New Winding Methods and Basic Winding Parameters," TAPPI Finishing and Converting Conference Proceedings, 1984.